Anomalous Nernst effect from a chiral d-density wave state in underdoped cuprate superconductors

Chuanwei Zhang[1,2], Sumanta Tewari[1,3], Victor M. Yakovenko[1], and S. Das Sarma[1]
[1]*Condensed Matter Theory Center, Department of Physics, University ofMaryland, College Park, Maryland 20742, USA*
[2]*Department of Physics and Astronomy, Washington State University, Pullman, WA 99164 USA*
[3]*Department of Physics and Astronomy, Clemson University, Clemson, SC 29634 USA*

We show that the breakdown of time-reversal invariance, confirmed by the recent polar Kerr effect measurements in the cuprates, implies the existence of an anomalous Nernst effect in the pseudogap phase of underdoped cuprate superconductors. Modeling the time-reversal-breaking ordered state by the chiral d-density-wave state, we find that the magnitude of the Nernst effect can be sizable even at temperatures much higher than the superconducting transition temperature. These results imply that the experimentally found Nernst effect at the pseudogap temperatures may be due to the chiral d-density wave ordered state with broken time-reversal invariance.

PACS numbers: 74.72.-h, 72.15.Jf, 72.10.Bg

I. INTRODUCTION

Even after two decades of intensive research, the physics of the high temperature cuprate superconductors is as elusive as ever[1]. The principal mystery surrounds the underdoped regime, which evinces a well-formed quasiparticle gap even at temperatures well above the superconducting transition temperature, T_c. The recent observation of a non-zero polar Kerr effect (PKE) in the underdoped YBCO[2], which demonstrates macroscopic time-reversal (TR) symmetry breaking in the pseudogap phase, is a step forward in solving the pseudogap puzzle. The PKE appears roughly at the same temperature, T^*, where the pseudogap develops[2]. Near optimum doping, the PKE appears at a temperature *below* T_c, consistent with the existence of a zero temperature quantum phase transition under the superconducting dome. This observation suggests that the TR symmetry breaking and the pseudogap in the cuprates may have the same physical origin, which is also unrelated to the d-wave superconductivity itself. Similar conclusion was also reached eariler by muon spin rotation experiments[3]. In this work we predict the existence of an anomalous Nernst effect associated with the TR symmetry breaking which should be present along with the observed PKE in the underdoped cuprates. Our results demonstrate that the existence of anomalous Nernst effect at temperatures as high as the pseudogap temperatures (see below), where the vortex excitations of the superconductor are unlikely to be present, may imply an ordered state with broken TR symmetry in the pseudogap regime of the underdoped cuprates.

It was proposed earlier[4,5] that the $id_{x^2-y^2}$ density-wave (DDW) state may be responsible for the pseudogap behavior in the underdoped cuprates. In real space, the order parameter for this state consists of orbital currents along the bonds of the two dimensional square lattice of Copper atoms. Since the currents circulate in opposite directions in any two consecutive unit cells of the lattice, the total orbital current averages to zero, and the macroscopic TR symmetry remains unbroken. Recently, it was shown that the admixture of a small d_{xy} component to the order parameter of the DDW state breaks the global TR symmetry, producing a non-zero Kerr signal[6] in conformity with the experiments[2]. The chiral $d_{xy} + id_{x^2-y^2}$ ($d + id$) density-wave state, as also the regular DDW and the spin density wave state, has hole and electron pockets as Fermi surfaces in its excitation spectra. Such reconstructed small Fermi pockets are consistent with the recently observed quantum oscillation in high magnetic fields in underdoped YBCO[7,8,9,10,11]. In this paper, we discuss an intrinsic anomalous Nernst effect induced by the $d + id$ density-wave state as a direct consequence of the macroscopic TR symmetry breaking and the presence of the Fermi pockets. Because of the broken TR symmetry, the ordered state acquires a Berry curvature[12] which is sizable on the Fermi surfaces. It is known that the non-zero Berry curvature can produce the anomalous Hall[13,14,15,16] and Nernst[17,18] effects in ferromagnets. We focus here on the anomalous Nernst effect for the high-T_c cuprates, because the corresponding coefficient has been extensively measured[19,20,21].

Nernst signal for unconventional density waves, such as the DDW state, was studied earlier in Ref. [22] and references therein. In these papers, however, the order parameter of the bare DDW state was used, for which the Nernst effect was induced by the external magnetic field. On the other hand, in the present paper we consider the superposition of two different d-wave order parameters (motivated by the PKE measurements[2,6]), and the spontaneous breakdown of time reversal symmetry leads to the Berry curvature, which acts as a magnetic field. Estimating the degree of TR symmetry breaking from the PKE measurements of Ref.[2], we calculate the expected anomalous Nernst signal in the underdoped phase of YBCO near T^*. We stress that even though we model the pseudogap by a chiral DDW state, the basic conclusions are more robust; the broken TR symmetry and well-defined Fermi surfaces, both of which have now been experimentally verified, necessarily imply the anomalous Nernst effect which should be observable. Note that, recent neutron scattering experiments[23,24] have appeared to indicate a TR breaking state without translational symmetry breaking in the pseudogap regime[25]. We expect an anomalous Nernst effect for such a state as well, if it breaks the TR symmetry globally.

II. BERRY CURVATURE OF THE CHIRAL DDW STATE

The order parameter of the $d_{xy} + id_{x^2-y^2}$ density wave state[26] is a combination of two density waves with different angular patterns

$$\left\langle c^{\dagger}_{\mathbf{k}+\mathbf{Q}\alpha} c_{\mathbf{k}\beta} \right\rangle = \left(\Delta_{\mathbf{k}} + iW_{\mathbf{k}}\right)\delta_{\alpha\beta}, \tag{1}$$

where $c^{\dagger}, c$ are the electron creation and annihilation operators on the 2D square lattice of Copper atoms, $\mathbf{k}$ is a 2D momentum, $\mathbf{Q}$ is the momentum space modulation vector (π, π), and α, β are the spin indices. $W_{\mathbf{k}} = \frac{W_0}{2}(\cos k_x - \cos k_y)$ and $\Delta_{\mathbf{k}} = -\Delta_0 \sin k_x \sin k_y$ are the order parameter amplitudes of the $id_{x^2-y^2}$ and d_{xy} density wave components, respectively. The imaginary part, $iW_{\mathbf{k}}$, of the order parameter breaks the microscopic TR symmetry giving rise to spontaneous currents along the nearest neighbor bonds of the square lattice. The spontaneous currents produce a staggered magnetic flux, which averages to zero on the macroscopic scale. The d_{xy} component of the density wave, $\Delta_{\mathbf{k}}$, leads to the staggered modulation of the diagonal electron tunneling between the next-nearest neighbor lattice sites. Such staggered modulation breaks the symmetry between the plaquettes with positive and negative circulation and, thus, breaks the macroscopic TR symmetry. Such macroscopic TR symmetry breaking may account for the nonzero PKE observed in the recent experiments[2,6].

The Hartree-Fock Hamiltonian appropriate for the mean-field $d + id$ density wave is given by

$$H = \sum_{\mathbf{k}\in RBZ} \Psi^{+}_{\mathbf{k}} \begin{pmatrix} \varepsilon_{\mathbf{k}} - \mu & D_{\mathbf{k}} \exp\left(i\theta_{\mathbf{k}}\right) \\ D_{\mathbf{k}} \exp\left(-i\theta_{\mathbf{k}}\right) & \varepsilon_{\mathbf{k}+\mathbf{Q}} - \mu \end{pmatrix} \Psi_{\mathbf{k}}, \tag{2}$$

where $\Psi^{+}_{\mathbf{k}} = \begin{pmatrix} c^{\dagger}_{\mathbf{k}} & c^{\dagger}_{\mathbf{k}+\mathbf{Q}} \end{pmatrix}$, $\varepsilon_{\mathbf{k}}$ is the free electron band structure, $\varepsilon_{\mathbf{k}} = -2t(\cos k_x + \cos k_y) + 4t' \cos k_x \cos k_y$, and μ is the chemical potential. The order parameter has been rewritten as $D_{\mathbf{k}} \exp\left(i\theta_{\mathbf{k}}\right)$ with the amplitude $D_{\mathbf{k}} = \sqrt{W^2_{\mathbf{k}} + \Delta^2_{\mathbf{k}}}$ and the phase $\theta_{\mathbf{k}} = \pi\Theta\left(-\Delta_{\mathbf{k}}\right) + \arctan\left(W_{\mathbf{k}}/\Delta_{\mathbf{k}}\right)$, where $\Theta\left(x\right)$ is the step function. In writing the Hamiltonian, the first Brillouin zone has been folded to the magnetic or reduced Brillouin zone (RBZ) to treat the $\mathbf{Q} = (\pi, \pi)$ modulation effectively. The energy spectrum of the Hamiltonian (2) contains two bands with eigenenergies $E_{\pm}\left(\mathbf{k}\right) = w_0 \pm w\left(\mathbf{k}\right)$, where $w_0\left(\mathbf{k}\right) = -\mu + \left(\varepsilon_{\mathbf{k}} + \varepsilon_{\mathbf{k}+\mathbf{Q}}\right)/2$, $w\left(\mathbf{k}\right) = \sqrt{F^2_{\mathbf{k}} + D^2_{\mathbf{k}}}$ with $F_{\mathbf{k}} = \left(\varepsilon_{\mathbf{k}} - \varepsilon_{\mathbf{k}+\mathbf{Q}}\right)/2$.

Berry phase is a geometric phase acquired by the wavefunction when the Hamiltonian of a physical system undergoes transformation along a closed contour in the parameter space[12]. For the $d + id$ Hamiltonian (2), the relevant parameter space is the space of the crystal momentum $\mathbf{k}$. The eigenfunctions of the Hamiltonian are therefore $\mathbf{k}$-dependent, and the overlap of two wavefunctions infinitesimally separated in the $\mathbf{k}$-space defines the Berry phase connection $\mathbf{A}_{\mathbf{k}} = \left\langle \Phi^{\dagger}_n\left(\mathbf{k}\right) \right| i\nabla_{\mathbf{k}} \left| \Phi_n\left(\mathbf{k}\right) \right\rangle$, where $\Phi_n\left(\mathbf{k}\right)$ is the periodic amplitude of the Block wave function, and n is the band index. The Berry phase connection corresponds to an effective vector potential in the momentum space, and its line integration around a close path gives the Berry phase. The Berry curvature, the Berry phase per unit area in the $\mathbf{k}$ space, is given by

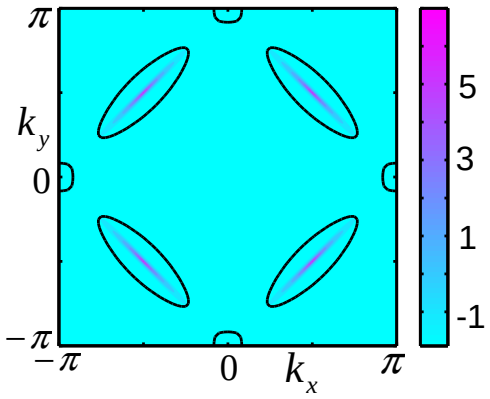

FIG. 1: (Color online) Logarithm of the Berry curvature $\Omega_{+}\left(\mathbf{k}\right)$ plotted on the Brillouin zone. The Berry curvature is sharply peaked at the points $(\pm\frac{\pi}{2}, \pm\frac{\pi}{2})$. The ellipses and the half-circles are the hole and the electron pockets of the $d + id$ state, respectively. $t = 0.3$ eV, $t' = 0.09$ eV, $\mu = -0.26$ eV, $W_0 = 0.08$ eV, $\Delta_0 = 0.004$ eV.

$$\mathbf{\Omega}_n\left(\mathbf{k}\right) = \nabla_{\mathbf{k}} \times \mathbf{A}_{\mathbf{k}}, \quad \mathbf{A}_{\mathbf{k}} = \left\langle \Phi^{\dagger}_n\left(\mathbf{k}\right) \right| i\nabla_{\mathbf{k}} \left| \Phi_n\left(\mathbf{k}\right) \right\rangle. \tag{3}$$

The Berry curvature $\mathbf{\Omega}_n\left(\mathbf{k}\right)$, thus, acts as an effective magnetic field in the momentum space and enters in the equations of motion of the wavepacket. For a system invariant under both time reversal and spatial inversion symmetries, the Berry curvature $\mathbf{\Omega}_n\left(\mathbf{k}\right) = 0$ for every $\mathbf{k}$. However, the $d + id$ density-wave state breaks the macroscopic TR symmetry, therefore the Berry curvature can acquire non-zero values.

To calculate the non-zero Berry curvature, we find the eigenstates of the Hamiltonian (2), which are given by $\Phi_{\pm}\left(\mathbf{k}\right) = \left(u_{\pm}\left(\mathbf{k}\right) e^{i\theta_{\mathbf{k}}/2}, v_{\pm}\left(\mathbf{k}\right) e^{-i\theta_{\mathbf{k}}/2}\right)$, where $+$ and $-$ correspond to the upper and lower bands with the energy dispersion $E_{+}\left(\mathbf{k}\right)$ and $E_{-}\left(\mathbf{k}\right)$, respectively. The coefficients $u_{\pm}\left(\mathbf{k}\right)$ and $v_{\pm}\left(\mathbf{k}\right)$ in the eigenstates $\Phi_{\pm}\left(\mathbf{k}\right)$ are straightforwardly obtained from the matrix (2). Substituting the eigenstates $\Phi_{\pm}\left(\mathbf{k}\right)$ into Eq. (3), we find $\mathbf{\Omega}_{\pm}\left(\mathbf{k}\right) = -\frac{1}{2}\nabla_{\mathbf{k}}\left(u^2_{\pm}\left(\mathbf{k}\right) - v^2_{\pm}\left(\mathbf{k}\right)\right) \times \nabla_{\mathbf{k}}\theta_{\mathbf{k}}$. In the pure DDW state, $\theta_{\mathbf{k}} = \pi/2$ is a constant, therefore $\mathbf{\Omega}_{\pm}\left(\mathbf{k}\right) = 0$ and there are no Berry phase effects. However, in the $d + id$ density-wave state, the phase $\theta_{\mathbf{k}} = \pi\Theta\left(-\Delta_{\mathbf{k}}\right) + \arctan\left(W_{\mathbf{k}}/\Delta_{\mathbf{k}}\right)$ depends on the values of order parameters W_k and Δ_k, and can vary in the $\mathbf{k}$ space, therefore $\mathbf{\Omega}_{\pm}\left(\mathbf{k}\right)$ can acquire nonzero values. Because the momentum $\mathbf{k}$ is restricted to the xy plane, only the z component of $\mathbf{\Omega}_{\pm}\left(\mathbf{k}\right)$ can be nonzero, which we will denote as $\Omega_{\pm}\left(\mathbf{k}\right)$. After some straightforward algebra, we find

$$\Omega_{\pm}\left(\mathbf{k}\right) = \mp\frac{1}{2w^3\left(\mathbf{k}\right)}\mathbf{w}_k \cdot \left[\frac{\partial \mathbf{w}_k}{\partial k_x} \times \frac{\partial \mathbf{w}_k}{\partial k_y}\right], \tag{4}$$

$$= \pm\frac{t\Delta_0 W_0}{w^3\left(\mathbf{k}\right)}\left(\sin^2 k_y + \cos^2 k_y \sin^2 k_x\right) \tag{5}$$

where $\mathbf{w}_{\mathbf{k}}$ is a three-component vector, $\mathbf{w}_{\mathbf{k}} = (-\Delta_{\mathbf{k}}, -W_{\mathbf{k}}, F_{\mathbf{k}})$, and it enters into the Hamiltonian density in (2) as $\hat{H} = w_0\hat{I} + \mathbf{w}_{\mathbf{k}} \cdot \hat{\tau}_{\mathbf{i}}$. Here $\hat{\tau}_{\mathbf{i}}$ $(i = 1, 2, 3)$

are the Pauli matrices and $\hat{I}$ is the 2×2 unit matrix operating on the spinors $\Psi_{\mathbf{k}}^{+}$, $\Psi_{\mathbf{k}}$. We see from Eq. (5) that the Berry curvature is nonzero only when the amplitudes Δ_0 and W_0 of the d_{xy} and $id_{x^2-y^2}$ order parameters are both nonzero. The Berry curvatures have opposite signs in the upper and the lower bands: $\Omega_+(\mathbf{k}) = -\Omega_-(\mathbf{k})$. In Fig. 1, we plot the Berry curvature Ω_+ with respect to the momentum $\mathbf{k}$ for a set of parameters in the $d+id$ state. We see that Ω_+ peaks at $\left(\pm\frac{\pi}{2}, \pm\frac{\pi}{2}\right)$, where $w(\mathbf{k})$ reaches the minimum and the corresponding points in the $\mathbf{k}$ space are the points of near degeneracy between the two bands. The value of Ω_+ decreases dramatically along slim ellipses whose long axes lay on the RBZ boundary lines $k_y \pm k_x = \pm\pi$ where $w(\mathbf{k})$ and the band splitting are the smallest. The peaks of the Berry curvature $\Omega_\pm$ correspond to magnetic monopoles in the momentum space[16].

III. ANOMALOUS NERNST EFFECT IN THE CHIRAL DDW STATE

In the experiments to observe Nernst effect[17,20,21], a temperature gradient $-\nabla T$, applied along, say, the $\hat{x}$ direction produces a measurable transverse electric field. The charge current along $\hat{x}$ driven by $-\nabla T$ is balanced by a backflow current produced by an electric field $\mathbf{E}$. The total charge current in the presence of $\mathbf{E}$ and $-\nabla T$ is thus given by, $J_i = \sigma_{ij}E_j + \alpha_{ij}(-\partial_j T)$, where σ_{ij} and α_{ij} are the electric and the thermoelectric conductivity tensors, respectively. In the experiments, $\mathbf{J}$ is set to zero and the Nernst signal, defined as

$$e_N \equiv E_y/|\nabla T| = \rho\alpha_{xy} - S\tan\theta_H, \tag{6}$$

is measured, where α_{xy} is Nernst conductivity defined via the relation $J_x = \alpha_{xy}(-\partial_y T)$ in the absence of the electric field, $\rho = 1/\sigma_{xx}$ is the longitudinal resistance, $S = E_x/|\nabla T| = \rho\alpha_{xx}$ is the thermopower, and $\tan\theta_H = \sigma_{xy}/\sigma_{xx}$ is the Hall angle. For a relatively modest hole concentration away from the severely underdoped regime in the cuprates, the second term in Eq. (6) is experimentally observed to be small[20]. As long as the second term is small, $\rho\alpha_{xy}$ completely defines the Nernst signal, but in the most general case one should extract α_{xy} from the experimental data, as it was done in Refs.[17,20], to compare with our theory.

The Berry-phase effects have found much success in explaining the anomalous Hall and Nernst effects in ferromagnets[13,16,17,18]. In the presence of an external electric field $\vec{E}$ along the $\hat{x}$ direction, the anomalous Hall current is along the transverse $\hat{y}$ direction. The anomalous DC Hall conductivity is found to be

$$\sigma_{xy} = -\frac{e^2}{\hbar}\int_{\mathrm{RBZ}}\frac{dk_x dk_y}{(2\pi)^2}\Omega_-\left[f\left(E_-(k)\right) - f\left(E_+(k)\right)\right], \tag{7}$$

where $f(E_n) = 1/(1+\exp(\beta E_n))$ is the Fermi distribution function at a temperature T, $\beta = 1/k_B T$ and we have used $\Omega_+ = -\Omega_-$. Eq. (7) agrees with the DC Hall conductivity of the $d+id$ density wave obtained earlier using a different approach[6,27,28]. For half filling ($t' = 0$, $\mu = 0$), when the system is a band insulator, its value is quantized, $e^2/2\pi\hbar$[27,28] per spin component. It changes continuously as the system deviates from half filling and the Fermi pockets appear[6]. We will see below that the anomalous Nernst effect is zero in the case of half filling and becomes non-zero only when there are hole and electron pockets in the spectrum.

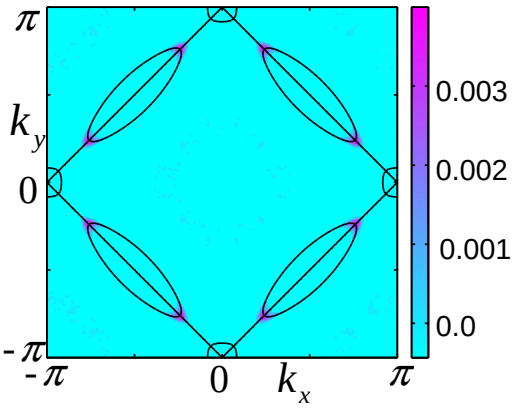

FIG. 2: (Color online) The contour plot of the integrand of Eq. (9) for the anomalous Nernst conductivity. The plotting parameters are the same as those in Fig. 1 except $\Delta_0 = 0.0008$ eV. $T = 130$ K. The main contribution to the anomalous Nernst signal comes from the lower band (hole pockets). The upper band (electron pockets) gives a negligible contribution.

In order to obtain the coefficient α_{xy}, it is more convenient to calculate the coeffecient $\bar{\alpha}_{xy}$, which determines the transverse heat current $\mathbf{J}^h$ in response to the electric field $\mathbf{E}$: $J_x^h = \bar{\alpha}_{xy}E_y$. It is related to α_{xy} by the Onsager relation $\bar{\alpha}_{xy} = T\alpha_{xy}$[18,29]. In the presence of the Berry curvature and the electric field, the electron velocity acquires the additional anomalous term $\hbar\mathbf{v}_{\mathbf{k}} = e\mathbf{E}\times\mathbf{\Omega}(\mathbf{k})$[17,18]. Multiplying this velocity by the entropy density of the electron gas, we obtain the coefficient for the transverse heat current:

$$\bar{\alpha}_{xy} = T\alpha_{xy} = \frac{e}{\beta\hbar}\sum_{n=\pm}\int_{\mathrm{RBZ}}\frac{dk_x dk_y}{(2\pi)^2}\Omega_n(\mathbf{k})\, s_n(\mathbf{k}). \tag{8}$$

Here $s(\mathbf{k}) = -f_{\mathbf{k}}\ln f_{\mathbf{k}} - (1-f_{\mathbf{k}})\ln(1-f_{\mathbf{k}})$ is the entropy density of the electron gas, $f_{\mathbf{k}} = f[E_n(\mathbf{k})]$ is the Fermi distribution function, and the sum is taken over both bands. Using the explicit expression for the Fermi distribution function, Eq. (8) can be transformed to the following form

$$\alpha_{xy} = \frac{e}{\hbar}\frac{1}{T}\sum_{n=\pm}\int_{\mathrm{RBZ}}\frac{dk_x dk_y}{(2\pi)^2}\Omega_n \times \left\{E_n(\mathbf{k})\, f\left(E_n(\mathbf{k})\right) - k_B T\log\left[1 - f\left(E_n(\mathbf{k})\right)\right]\right\}. \tag{9}$$

Eq. (9) coincides with the corresponding expression derived in Ref.[18] using the semiclassical wavepacket methods and taking into accound the orbital magnetization of the carriers[30]. Relation of the transverse heat current to the entropy flow was also discussed in Refs.[29] and[17]. At $T = 0$, the carrier entropy is zero, $s_n(\mathbf{k}) = 0$, so there is no heat current and $\alpha_{xy} = 0$. At $T \neq 0$, we first consider the simple case with $t' = 0$ and

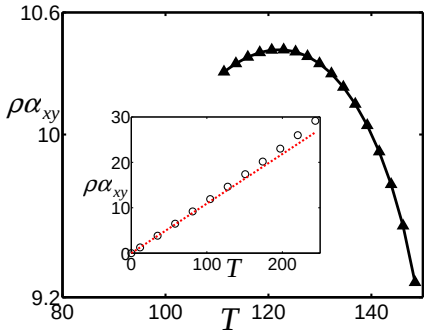

FIG. 3: (Color online) Plot of the Nernst signal, see Eq. (6), versus temperature T. The unit on the y-axis is nV/K. The inset, with temperature independent order parameters $W_0 = 0.08$ eV, $\Delta_0 = 0.1\% W_0$ eV, shows that the Nernst signal satisfies the Mott relation (10). In the inset, dotted line corresponds to the Mott relation (10) and the open circles are obtained through numerical integration of Eq. (9).

$\mu = 0$, that is, the lower and the upper bands are symmetric with $E_+(\mathbf{k}) = -E_-(\mathbf{k})$. It is easy to check that in this case $\alpha_{xy} = 0$ because $\Omega_+ = -\Omega_-$.

In the general case, the entropy $s_n(\mathbf{k})$ has peaks on the Fermi surface and decreases dramatically away from the Fermi surface. Because the Berry curvature $\Omega_\pm$ peaks along the RBZ boundary $k_x \pm k_y = \pm\pi$, the integrand in Eq. (9) peaks at the intersections of the Fermi surface and the RBZ boundary, the so called "hot spots"[31,32], which were shown earlier to be important in the calculations of the Hall coefficient in the DDW state[33]. These peaks are clearly seen in Fig. 2.

From Eqs. (7), (8), and (9), we can show that, at low temperatures, the Nernst conductivity α_{xy} is related to the zero temperature Hall conductivity σ_{xy} through the Mott relation[34], which yields

$$\alpha_{xy} = \frac{\pi^2 k_B^2}{3e} \frac{d\sigma_{xy}}{d\mu} T. \tag{10}$$

Here the derivative of σ_{xy} leads to $\frac{d\sigma_{xy}}{d\mu} = -\frac{e^2}{\hbar}\int_{\mathrm{RBZ}} \frac{dk_x dk_y}{(2\pi)^2}\Omega_- [\delta(E_-) - \delta(E_+)]$. Here $\delta(E_\pm)$ are the delta functions. Therefore the integrand is nonzero only at the boundary lines of the hole and electron pockets. In the case of a band insulator ($t' = 0$, $\mu = 0$) that does not contain the Fermi pockets, $\sigma'_{xy}(\mu) = 0$ and the anomalous Nernst conductivity $\alpha_{xy} = 0$, even though the DC Hall conductivity, Eq. (7), is non-zero and, in fact, is quantized[6]. This is because the quantum Hall current carries no entropy.

For crude estimate of the Nernst signal, we choose a set of parameters appropriate for the underdoped YBCO[35], $t = 0.3$ eV, $t' = 0.09$ eV, $\mu = -0.26$ eV (corresponding to the hole doping of about 10%), $d = 1.17$ nm (the distance between consecutive 2D layers), $\rho = 3$ mΩcm, $W_0(T) = 0.1\left(1 - T/T^*_W\right)^{1/2}$ eV, $\Delta_0(T) = 0.0001\left(1 - T/T^*_\Delta\right)^{1/2}$ eV, and numerically integrate Eq. (9), where we made reasonable assumptions about the transition temperatures, $T^*_W \approx 150$ K[2] and $T^*_\Delta \approx 250$ K. In Fig. 3, we plot $\rho\alpha_{xy}$ in a temperature regime that is below T^*_W but much higher than the superconducting transition temperature $T_c \approx 80$ K[2]. Here we have multiplied the results by 2 to account for the contributions from two spin components. As temperature drops from T^*_W, the order parameter $W_0(T)$ grows, leading to the increase of the Nernst signal. Close to T_c, the Nernst effect would be dominated by the mobile vortices and our calculations do not apply there. The estimated value of $\rho\alpha_{xy}$ at $T \sim 130$ K is about 10 nV/K. This value is about 10% of the experimentally observed Nernst signals in underdoped LSCO and BSCCO[21] at temperatures much higher than the superconducting T_c. Note that the spontaneous Nernst signal discussed above may not be observable through the DC current measurements[21] without a non-zero magnetic field because of the macroscopic domains with opposite chiralities present in a sample at the zero magnetic field.

IV. CONCLUSION

In summary, we discuss the non-zero Berry curvature in the $d + id$ density-wave state, which was proposed earlier[6] to explain the time-reversal symmetry breaking[2] in the pseudogap phase of the high T_c superconductor YBCO. We show that the nonzero Berry curvature, arising out of the broken time-reversal invariance, and the existence of Fermi pockets in the cuprates directly imply an anomalous Nernst effect which should be measurable. We note that measurable Nernst signals have been found in underdoped LSCO and BSCCO[21] even at temperatures much higher than T_c, and we propose that a TRS breaking state, such as the chiral DDW state, may be the origin of these signals. The anomalous Nernst effect at the pseudogap temperatures will constitute a further proof of an ordered state, with broken time-reversal invariance, to be responsible for the pseudogap phenomena in the cuprates.

This work is supported by ARO-DARPA and LPS-CMTC.

[1] P. A. Lee, N. Nagaosa, and X.-G. Wen, Rev. Mod. Phys. **78**, 17 (2006).

[2] J. Xia, E. Schemm, G. Deutscher, S. A. Kivelson, D. A. Bonn, W. N. Hardy, R. Liang, W. Siemons, G. Koster, M. M. Fejer, and A. Kapitulnik, Phys. Rev. Lett. **100**, 127002 (2008).

[3] J. E. Sonier, J. H. Brewer, R. F. Kiefl, R. I. Miller, G. D. Morris, C. E. Stronach, J. S. Gardner, S. R. Dunsiger, D. A. Bonn, W. N. Hardy, R. Liang, and R. H. Heffner, Science **292**, 1692 (2001).

[4] S. Chakravarty, R. B. Laughlin, D. K. Morr, and C. Nayak, Phys. Rev. B **63**, 094503 (2001).

[5] S. Chakravarty, H.-Y. Kee and K. Völker, Nature **428**, 53 (2004).

[6] S. Tewari, C. Zhang, V. M. Yakovenko, and S. Das Sarma, Phys. Rev. Lett. **100**, 217004 (2008).

[7] N. Doiron-Leyraud, C. Proust, D. LeBoeuf, J. Levallois, J.-B.

Bonnemaison, R. Liang, D. A. Bonn, W. N. Hardy and L. Taillefer, Nature **447**, 565 (2007).
[8] E. A. Yelland, J. Singleton, C. H. Mielke, N. Harrison, F. F. Balakirev, B. Dabrowski, and J. R. Cooper, Phys. Rev. Lett. **100**, 047003 (2008).
[9] A. F. Bangura, J. D. Fletcher, A. Carrington, J. Levallois, M. Nardone, B. Vignolle, P. J. Heard, N. Doiron-Leyraud, D. LeBoeuf, L. Taillefer, S. Adachi, C. Proust, and N. E. Hussey, Phys. Rev. Lett. **100**, 047004 (2008).
[10] C. Jaudet, D. Vignolles, A. Audouard, J. Levallois, D. LeBoeuf, N. Doiron-Leyraud, B. Vignolle, M. Nardone, A. Zitouni, R. Liang, D. A. Bonn, W. N. Hardy, Louis Taillefer, and C. Proust, Phys. Rev. Lett. **100**, 187005 (2008).
[11] S. Chakravarty and H.-Y. Kee, Proc. Natl. Acad. Sci. USA **105**, 8835 (2008).
[12] M. V. Berry, Proc. R. Soc. London A **392**, 92 (2003).
[13] Y. Taguchi, Y. Taguchi, Y. Oohara, H. Yoshizawa, N. Nagaosa, and Y. Tokura, Science **291**, 2573 (2001).
[14] W.-L. Lee, S. Watauchi, V. L. Miller, R. J. Cava, and N. P. Ong, Science **303**, 1647 (2004).
[15] T. Jungwirth, Q. Niu, and A. H. MacDonald, Phys. Rev. Lett. **88**, 207208 (2002).
[16] Z. Fang, N. Nagaosa, K. S. Takahashi, A. Asamitsu, R. Mathieu, T. Ogasawara, H. Yamada, M. Kawasaki, Y. Tokura, and K. Terakura, Science **302**, 92 (2003);
[17] W.-L. Lee, S. Watauchi, V. L. Miller, R. J. Cava, and N. P. Ong, Phys. Rev. Lett. **93**, 226601 (2004).
[18] D. Xiao, Y. Yao, Z. Fang, and Q. Niu, Phys. Rev. Lett. **97**, 026603 (2006).
[19] Z. A. Xu, N. P. Ong, Y. Wang, T. Kakeshita, and S. Uchida, Nature **406**, 486 (2000).
[20] Y. Wang, Z. A. Xu, T. Kakeshita, S. Uchida, S. Ono, Yoichi Ando, and N. P. Ong, Phys. Rev. B. **64**, 224519 (2001).
[21] Y. Wang, L. Li, and N. P. Ong, Phys. Rev. B, **73**, 024510 (2006).
[22] B. Dóra, K. Maki, A. Virosztek, and A. Ványolos, Phys. Rev. B **71**, 172502 (2005)
[23] B. Fauque, Y. Sidis, V. Hinkov, S. Pailhès, C. T. Lin, X. Chaud, and P. Bourges, Phys. Rev. Lett. **96**, 197001 (2006).
[24] H. A. Mook, Y. Sidis, B. Fauqué, V. Balédent, and P. Bourges, Phys. Rev. B **78**, 020506(R) (2008).
[25] M. E. Simon and C. M. Varma, Phys. Rev. Lett. **89**, 247003 (2002).
[26] C. Nayak, Phys. Rev. B **62**, 4880 (2000).
[27] V. M. Yakovenko, Phys. Rev. Lett. **65**, 251 (1990).
[28] P. Kotetes, G. Varelogiannis, and P.B. Littlewood, arXiv:0802.4080.
[29] N. R. Cooper, B. I. Halperin, and I. M. Ruzin, Phys. Rev. B **55**, 2344 (1997).
[30] J. Shi, G. Vignale, D. Xiao, and Q. Niu, Phys. Rev. Lett. **99**, 197202 (2007).
[31] R. Hlubina and T. M. Rice, Phys. Rev. B **51**, 9253 (1995).
[32] B. P. Stojkovic and D. Pines, Phys. Rev. Lett. **76**, 811 (1996).
[33] S. Chakravarty, C. Nayak, S. Tewari, and X. Yang, Phys. Rev. Lett. **89**, 277003 (2002).
[34] M. P. Marder, *Condensed Matter Physics*, Wiley, New York, (2000).
[35] O. K. Anderson, A. I. Liechtenstein, O. Jepsen, and F. Paulsen, J. Phys. Chem. Solids **56**, 1573 (1995).